Synthesis and Structure Characterization of Liquid Crystalline Polyacrylates with Unconventional Fluoroalkylphenyl Mesogens

Luisa Andruzzi,[†] Francesca D'Apollo,[†] Giancarlo Galli,*[,†] and Bernard Gallot[‡]

Dipartimento di Chimica e Chimica Industriale, Università di Pisa, 56126 Pisa, Italy; and Laboratoire des Matériaux Organiques à Propriétes Spécifiques, CNRS, 69390 Vernaison, France

Received April 30, 2001; Revised Manuscript Received August 17, 2001

ABSTRACT: The synthesis, thermal behavior, and bulk microstructure of fluorinated new liquid-crystalline polyacrylates containing spaced fluoroalkylphenyl units in the side chains were studied. While in polyacrylates poly**(1)** and poly**(2)** there was a 4-(perfluorooctylethoxy)phenyl benzoate unit, i.e., a two-phenyl mesogenic core, poly**(3)** contained a 4-perfluorooctylethyl benzoate, i.e., a one-phenyl aromatic core that per se would not be able to promote a thermotropic behavior. X-ray diffraction studies allowed identification of the mesophases (hexatic smectic, disordered smectic, nematic) and study of the evolution of their structures and lattice parameters with temperature. It was found that each polymer presented a rich mesophase polymorphism, including the rather unusual smectic F_2- (or I_2-) to-nematic transition in poly**(3)**. The electron density profiles along the smectic layer normal were drawn and provided a deeper insight into the packing of the side chains in tilted double layer structures. The strong mesogenic character of the polymers was attributed to the presence of the fluorinated tail on the aromatic core owing to its capability of adopting a rigid-rodlike conformation. A phase separation occurring at the molecular level of the different incompatible aliphatic−aromatic−fluoroaliphatic sections of the polymer repeat unit should efficiently cooperate to the onset of thermotropic mesomorphism.

Introduction

Fluorinated liquid-crystalline polymers are a relatively new class of fluoropolymers.[1−9] Their useful properties such as low refractive index, low dielectric constant, and low surface energy can favor application in different fields ranging from optics to coatings.[10]

Initial studies on fluorinated liquid crystals focused on partly fluorinated alkanes, namely diblock hydrocarbon−fluorocarbon molecules such as $H(CH_2)_x(CF_2)_yF$ (x, $y \geq 6$).[11−15] The ability of these compounds to show the formation of liquid-crystalline mesophases was observed, presumably due to the strong phase separation of fluorocarbon from hydrocarbon chain segments[16] and also to the rigid-rodlike nature of the fluorocarbon chains which tend to adopt a helical conformation in the mesophase state.[17,18] Later synthetic efforts resulted in the realization of liquid-crystalline polymers in which the length of the fluorinated tail was varied over a wide range of numbers x and y.[1,3,5−7,9] Thus, appropriately fluorinated molecules may be regarded to as unconventional mesogens in that they do not possess the usual molecular features of more traditional liquid crystals. The latter molecules, in fact, are typified by core structures composed of two or more aromatic or cycloaliphatic rings, or combinations of them, that are either directly linked together, as, e.g., in biphenyls, or interconnected by a bridging group, as, e.g., an ester group in phenyl benzoates. Alkyl tails are also normally attached at both ends of the mesogenic core to introduce flexibility in the molecule and help tailor the mesophase transitions and properties of the materials.[19] More conventional mesogenic units, e.g., biphenyls, have also been used in combination with partly fluorinated tails in low-molar-mass[20−25] and polymeric liquid crystals.[8] However, comparatively little attention has been devoted to incorporating fluoroalkyl tails bridged with short methylene segments ($x < 3$) into any kind of fluorinated mesogens.[1,8,22−27]

Liquid-crystallinity may provide a useful tool while devising low surface energy polymeric materials for nonstick coating application.[6,7] It is envisaged that, from a molecular level perspective, a uniformly organized array of CF_3 groups would form a film surface with the lowest possible surface tension.[28] However, the poor stability of the surface properties of amorphous fluorinated polymers making the fluorinated side chains escape from the surface and hide in the bulk of the coating, when interfaced to a polar medium, represents a serious practical limitation in the utilization of these materials. The attachment of a fluorinated mesogen pendent to a polymer backbone can also bring about improvement and temporal stabilization of the surface upon exposure to different environments, as a consequence of the induced mesomorphic behavior in the bulk of the material. For example, investigations on block copolymers containing a fluorinated polymer block showed that rigid-rodlike fluorinated groups can form a highly organized surface structure, stable to reconstruction upon exposure to water as a consequence of the ordering of the fluorinated groups in a liquid-crystalline, smectic mesophase.[6] In fact, the fluorinated side groups of these polymers residing in a smectic mesophase while covering the surface of a polymer film should pay a too high enthalpy penalty to rearrange when in contact with water.

In pursuing this approach to the creation of stable, low surface energy films from fluorinated polymers, the main objective of the present contribution was the synthesis and characterization of the mesophase structure of new fluorinated liquid-crystalline polyacrylates poly**(1)**, poly**(2),** and poly**(3)** containing fluoroalkylphenyl mesogens.

* Author for correspondence. E-mail: gallig@dcci.unipi.it.
[†] Università di Pisa.
[‡] Laboratoire des Matériaux Organiques à Propriétes Spécifiques, CNRS.

10.1021/ma010728f CCC: $20.00
Published on Web 09/29/2001

Scheme 1

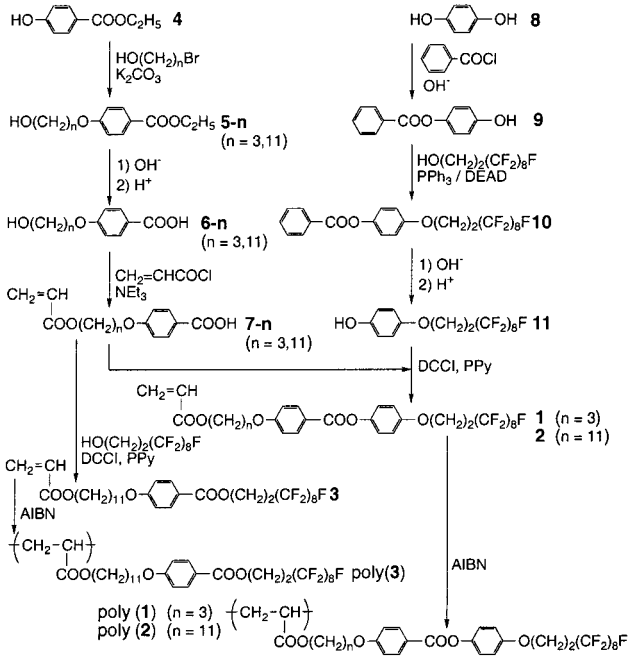

The former two polymers were composed of a two-phenyl group differently spaced by a $(CH_2)_n$ segment from the main chain ($n = 3$ or 11), while in the latter polymer there was just a one-phenyl group ($n = 11$). In each case, the fluorinated tail was a perfluorooctylethyl chain ($x = 2$, $y = 8$). It was found that in particular, poly**(3)** exhibited an unusual phase behavior that was attributed to its mixed aliphatic−aromatic−fluoroaliphatic character. The surface structure and properties of polymer films therefrom will be presented in a forthcoming paper.

Experimental Section

Starting Materials. Perfluorooctylethanol, triphenyl phosphine, diethyl azodicarboxylate (DEAD), hydroquinone, ethyl 4-hydroxybenzoate, 11-bromo-1-undecanol, 3-bromo-1-propanol, and 1,1,2-trifluorotrichloroethane were purchased from Aldrich and used without further purification. Acryloyl chloride was distilled under nitrogen atmosphere at 96 °C immediately prior to use. Triethylamine was refluxed over KOH and distilled under nitrogen atmosphere at 88 °C. Azobis(isobutyronitrile) was recrystallized from methanol.

Diethyl ether and tetrahydrofuran were refluxed over Na/K alloy and distilled under nitrogen. Trifluorotoluene was dried over Na_2SO_4 and distilled under dry nitrogen. 2-Butanone was dried over Na_2SO_4 and distilled over $KMnO_4$. Dichloromethane was distilled under nitrogen over P_2O_5.

Synthesis of Monomers. The syntheses of 4-perfluorooctylethoxyphenyl 4-(3-acryloyloxypropoxy)benzoate **(1)**, as a typical example, and of 4-perfluorooctylethyl 4-(11-acryloyloxyundecyloxy)benzoate **(3)** are described in detail (Scheme 1).

Ethyl 4-(3-Hydroxypropoxy)benzoate (5—3). A mixture of 100 mL of dry 2-butanone, 8.2 g (0.078 mol) of anhydrous K_2CO_3 and 8.7 g (0.052 mol) of ethyl 4-hydroxybenzoate **(4)** was heated to 80 °C under dry nitrogen atmosphere. Then a solution of 8.0 g (0.057 mol) of 1-bromo-3-propanol in 8 mL of 2-butanone was slowly added to the refluxing mixture, and afterward the reaction mixture was refluxed for an additional 48 h. It was then cooled and filtered to eliminate the inorganic products. The solvent was then evaporated to dryness under vacuum, and the crude product was recrystallized from ethanol. A total of 11.5 g (yield 98%) of **5—3** was obtained.

^{1}H NMR ($CDCl_3$, δ in ppm): 1.3 (3H, CH_3), 2.0 (3H, CH_2 + OH), 3.8 (2H, CH_2OH), 4.1 (2H, CH_2OPh), 4.3 (2H, CH_2OOC), 6.9 (2H, aromatic), 7.9 (2H, aromatic).

IR (KBr pellet, $\bar{\nu}$ in cm^{-1}) = 3500 (ν O−H), 3100−3050 (ν C−H aromatic), 2980−2840 (ν CH_2 and CH_3), 1720 (ν C═O), 1600−1450 (ν C═C aromatic, δ CH_2 and CH_3), 1280−1040 (ν C−O−C), 710 (δ C−H aromatic).

4-(3-Hydroxypropoxy)benzoic Acid (6—3). An 11.5 g (0.051 mol) sample of **5—3**, 125 mL of water, 175 mL of ethanol, and 4.2 g (0.075 mol) of KOH were refluxed for 6 h. After cooling to room temperature, the reaction mixture was acidified with 37% HCl to pH ≈ 2 and extracted with CH_2Cl_2. The organic solution was then dried over Na_2SO_4 and the solvent evaporated to dryness. The crude product residue was recrystallized from methanol giving 10.4 g (yield 97%) of **6—3**.

^{1}H NMR (DMSO-d_6, δ in ppm): 1.8 (2H, CH_2), 3.5 (2H, CH_2-OH), 4.1 (2H, CH_2OPh), 7.0 (2H, aromatic), 7.9 (2H, aromatic).

IR (KBr pellet, $\bar{\nu}$ in cm^{-1}) = 3500 (ν O−H), 3100−3050 (ν C−H aromatic), 2980−2840 (ν CH_2), 1710 (ν C═O), 1600−1450 (ν C═C aromatic, δ CH_2), 1250−1040 (ν C−O−C), 710 (δ C−H aromatic).

4-(3-Acryloyloxypropoxy)benzoic Acid (7—3). A solution of 5.5 g (0.028 mol) of **6—3**, 5.6 g (0.056 mol) of triethylamine, and 5 mg of 2,6-di-*tert*-butyl-4-cresol in 150 mL of anhydrous tetrahydrofuran was cooled to 0 °C under nitrogen atmosphere. Then 3.3 g (0.037 mol) of acryloyl chloride was slowly added under stirring. The reaction was continued for an additional 16 h at room temperature and 3 h at 45 °C. Finally, the solvent was evaporated under vacuum and the solid residue was dissolved in $CHCl_3$. The organic phase was washed with 5% HCl, water and dried over Na_2SO_4. After removal under vacuum of the solvent, the crude product was purified by silica gel column chromatography using an ethyl acetate/hexane (1/1 v/v) mixture as the eluent. A total of 2.0 g (yield 30%) of pure **7—3** was obtained (mp 122−124 °C).

^{1}H NMR ($CDCl_3$, δ in ppm): 2.1 (2H, CH_2), 4.1 (2H, CH_2-OPh), 4.5 (2H, CH_2OOC), 5.8 (1H, CH = trans), 6.2 (1H, CH = gem), 6.5 (1H, CH = cis), 7.0 (2H, aromatic), 7.9 (2H, aromatic).

IR (KBr pellet, $\bar{\nu}$ in cm^{-1}) = 3600 (ν O−H), 3100−3050 (ν C−H aromatic), 2980−2840 (ν CH_2 and CH_3), 1710 (ν C═O), 1620−1450 (ν C═C aromatic and vinyl, δ CH_2), 1250−1040 (ν C−O−C), 710 (δ C−H aromatic).

4-Hydroxyphenyl Benzoate (9). A solution of 300 mL of water, 7.6 g (0.14 mol) of KOH, and 20.0 g (0.18 mol) of hydroquinone **(8)** was cooled to 0 °C and 19.0 g (0.13 mol) of benzoyl chloride was slowly added under vigorous stirring. The mixture was then kept under stirring at 0 °C for 1 h and subsequently poured into 400 mL of a $NaHCO_3$ saturated solution and stirred for additional 30 min. The precipitate was filtered, washed with water and vacuum-dried. The crude product was purified by crystallization from 70% aqueous ethanol. A total of 15.2 g (yield 53%) of pure **9** was obtained (mp 163−165 °C).

^{1}H NMR (DMSO-d_6, δ in ppm): 9.5 (1H, OH), 8.2 (2H, aromatic), 7.7 and 7.6 (3H, aromatic), 7.1 (2H, aromatic), 6.9 (2H, aromatic).

IR (KBr pellet, $\bar{\nu}$ in cm^{-1}) = 3450 (ν O−H), 3100−3050 (ν C−H aromatic), 1714 (ν C═O), 1560, 1510, and 1450 (ν C═C aromatic), 1280−1210 (ν ArC−O), 1000 (δ C-H aromatic), 710 (δ C−H aromatic).

4-(Perfluorooctylethoxy)phenyl Benzoate (10). A solution of 6.3 g (0.036 mol) of diethyl azodicarboxylate (DEAD) in 10 mL of anhydrous diethyl ether was slowly added under vigorous stirring to a mixture of 6.9 g (0.032 mol) of **9**, 8.4 g (0.032 mol) of triphenyl phosphine, 15.0 g (0.032 mol) of perfluorooctylethanol, and 250 mL of anhydrous diethyl ether. The reaction mixture was kept at room temperature for 72 h. The precipitate formed during the reaction was filtered off and the solvent was evaporated under vacuum. The crude product was purified by silica gel column chromatography with ethyl acetate/hexane ($^1/_3$ v/v) as the eluent. A total of 2.7 g (yield 15%) of pure **10** was obtained (mp 68−71 °C).

^{1}H NMR ($CDCl_3$, δ in ppm): 2.6 (2H, CH_2CF_2), 4.3 (2H, CH_2-OPh), 6.9 (2H, aromatic), 7.2 (2H, aromatic), 7.5 (3H, aromatic), 8.2 (2H, aromatic).

4-(Perfluorooctylethoxy)phenol (11). A mixture of 2.7 g (4.09 mmol) of **10**, 0.6 g (0.011 mmol) of KOH, 20 mL of

water, and 40 mL of ethanol was refluxed for 6 h. The reaction mixture was then cooled, acidified with 37% HCl to pH ≈ 2, and extracted with CH_2Cl_2. The organic extracts were finally washed with 5% $NaHCO_3$ and 37% HCl. After evaporation of the solvent under vacuum, 1.9 g (88% yield) of pure **11** was obtained (mp 103−104 °C).

^{1}H NMR ($CDCl_3$, δ in ppm): 2.6 (2H, CH_2CF_2), 4.2 (2H, CH_2-OPh), 4.6 (1H, OH), 6.8 (4H, aromatic).

4-Perfluorooctylethoxyphenyl 4-(3-Acryloyloxypropoxy)benzoate (1). A solution of 1.8 g (3.2 mmol) of **11**, 0.8 g (3.21 mmol) of **7—3**, 0.05 g (0.36 mmol) of pyrrolidinopyridine (PPy), and 150 mL of anhydrous CH_2Cl_2 was stirred at room temperature for 30 min. Then a solution of 0.9 g (4.48 mmol) of dicyclohexyl carbodiimide (DCCI) in 15 mL of anhydrous CH_2Cl_2 was slowly added. The reaction mixture was kept under stirring at room temperature for 48 h. The precipitate formed during the reaction was filtered off and the organic solution was washed with 5% HCl, 5% $NaHCO_3$, water and dried over Na_2SO_4. The solvent was evaporated under vacuum and the crude product was purified by silica gel column chromatography using an ethyl acetate/hexane ($^1/_3$ v/v) mixture as the eluent and finally recrystallized from methanol. A total of 1.1 g (yield 45%) of pure **1** was obtained (mp 91−92 °C).

^{1}H NMR ($CDCl_3$, δ in ppm): 2.2 (2H, aliphatic CH_2), 2.6 (2H, CH_2CF_2), 4.1 and 4.2 (4H, CH_2OPh), 4.3 (2H, CH_2OOC), 5.8 (1H, CH = trans), 6.2 (1H, CH = gem), 6.4 (1H, CH = cis), 6.9 (4H, aromatic), 7.1 (2H, aromatic), 8.1 (2H, aromatic).

IR (KBr pellet, $\bar{\nu}$ in cm^{-1}) = 3100−3050 (ν C−H aromatic), 2980−2840 (ν CH_2), 1720 (ν C=O), 1680−1450 (ν C=C aromatic and vinyl, δ CH_2), 1250−1040 (ν C−O−C), 710 (δ C−H aromatic), 645 (ω CF_2).

^{19}F NMR ($CDCl_3$, δ in ppm): −5 (3F, CF_3), −37 (2F, CF_2), −45 to −50 (12F, 6 CF_2).

Anal. Calcd ($C_{30}H_{21}F_{17}O_7$): C, 44.13; H, 2.59; F, 39.56. Found: C, 44.08; H, 2.60; F, 39.7.

4-Perfluorooctylethoxyphenyl 4-(11-Acryloyloxyundecyloxy)benzoate (2). It was prepared according to the same synthetic procedure as for monomers **1**.

^{1}H NMR ($CDCl_3$, δ in ppm): 1.2−1.9 (18H, aliphatic CH_2), 2.6 (2H, CH_2CF_2), 4.0 and 4.2 (4H, CH_2OPh), 4.3 (2H, CH_2-OOC), 5.8 (1H, CH = trans), 6.1 (1H, CH = gem), 6.4 (1H, CH = cis), 6.9 (4H, aromatic), 7.1 (2H, aromatic), 8.1 (2H, aromatic).

IR (KBr pellet, $\bar{\nu}$ in cm^{-1}) = 3100−3050 (ν C−H aromatic), 2980−2840 (ν CH_2), 1720 (ν C=O), 1680−1450 (ν C=C aromatic and vinyl, δ CH_2), 1250−1040 (ν C−O−C), 710 (δ C−H aromatic), 646 (ω CF_2).

^{19}F NMR ($CDCl_3$, δ in ppm): −5 (3F, CF_3), −37 (2F, CF_2), −45 to −50 (12F, 6 CF_2).

Anal. Calcd ($C_{38}H_{37}F_{17}O_7$): C, 49.15; H, 4.02; F, 34.78. Found: C, 49.08; H, 4.10; F, 35.0.

Ethyl 4-(11-Hydroxyundecyloxy)benzoate (5—11). A mixture of 135 mL of anhydrous 2-butanone, 7.2 g (0.068 mol) of anhydrous K_2CO_3 and 7.5 g (0.045 mol) of **4** was heated to 80 °C under dry nitrogen atmosphere. A solution of 12.0 g (0.05 mol) of 1-bromo-11-undecanol in 25 mL of 2-butanone was slowly added and afterward the reaction mixture was refluxed for an additional 48 h. The mixture was then cooled and filtered to eliminate the inorganic products. After removal of the solvent under vacuum, 14.8 g (98% yield) of **5—11** was obtained.

^{1}H NMR ($CDCl_3$, δ in ppm): 1.1−1.8 (21H, aliphatic), 3.6 (2H, CH_2OH), 4.1 (2H, CH_2OPh), 4.4 (2H, CH_2OOC), 6.9 (2H, aromatic), 7.9 (2H, aromatic).

IR (KBr pellet, $\bar{\nu}$ in cm^{-1}) = 3500 (ν O−H), 3100−3050 (ν C−H aromatic), 2980−2840 (ν CH_2 and CH_3), 1720 (ν C=O), 1600−1450 (ν C=C aromatic), 1280−1040 (ν C−O−C), 720 (ρ CH_2), 710 (δ C−H aromatic).

4-(11-Hydroxyundecyloxy)benzoic Acid (6—11). A 14.0 g (0.041 mol) sample of **5—11**, 100 mL of water, 140 mL of ethanol, and 3.4 g (0.06 mol) of KOH were refluxed for 6 h. After cooling to room temperature, the reaction mixture was acidified with 37% HCl to pH ≈ 3 and the precipitate formed was filtered off. The crude product was recrystallized from methanol, and 13.2 g (98% yield) of **6—11** was obtained.

^{1}H NMR (DMSO-d_6, δ in ppm): 1.1−1.8 (18H, aliphatic), 3.4 (3H, CH_2OH), 4.1 (2H, CH_2OPh), 4.4 (1H, COOH), 7.0 (d, 2H, aromatic), 7.9 (2H, aromatic).

IR (KBr pellet, $\bar{\nu}$ in cm^{-1}) = 3500 (ν O−H), 3100−3050 (ν C−H aromatic), 2980−2840 (ν CH_2), 1720 (ν C=O), 1600−1450 (ν C=C aromatic), 1250−1040 (ν C−O−C), 720 (ρ CH_2), 710 (δ C−H aromatic).

4-(11-Acryloyloxyundecyloxy)benzoic Acid (7—11). A solution of 10.0 g (0.032 mol) of **6—11**, 6.2 g (0.065 mol) of triethylamine, and 5 mg of 2,6-di-*tert*-butyl-4-cresol in 150 mL of anhydrous tetrahydrofuran was cooled to 0 °C under nitrogen atmosphere. 3.7 g (0.04 mol) of acryloyl chloride was then slowly added under stirring. The reaction was continued for 16 h at room temperature and finally the solvent was evaporated under vacuum. The solid residue was dissolved in $CHCl_3$, washed with 5% HCl and water to neutrality and finally dried over Na_2SO_4. After removal of the solvent under vacuum, the solid residue was purified by silica gel column chromatography using an ethyl acetate/hexane ($^1/_2$ v/v) mixture as the eluent. 2.8 g (30% yield) of pure **7—11** was obtained (mp 101−102 °C).

^{1}H NMR ($CDCl_3$, δ in ppm): 0.9−2.1 (18H, 9CH_2), 4.1 (2H, CH_2OPh) 4.2 (2H, CH_2OOC), 5.8 (1H, CH = trans), 6.1 (1H, CH = gem), 6.4 (1H, CH = cis), 6.9 (2H, aromatic), 8.1 (2H, aromatic).

IR (KBr pellet, $\bar{\nu}$ in cm^{-1}) = 3600 (ν O−H), 3100−3050 (ν C−H aromatic), 2980−2840 (ν CH_2), 1720 (ν C=O), 1680−1450 (ν C=C aromatic and vinyl), 1250−1040 (ν C−O−C), 720 (ρ CH_2), 710 (δ C−H aromatic).

4-Perfluorooctylethyl 4-(11-Acryloyloxyundecyloxy)-benzoate (3). A mixture of 2.6 g (5.5 mmol) of perfluorooctylethanol, 2.0 g (5.5 mmol) of **7—11**, 0.19 g (1.2 mmol) of pyrrolidinopyridine (PPy), and 100 mL of anhydrous CH_2Cl_2 was stirred at room temperature. A solution of 1.5 g (7.1 mmol) of dicyclohexyl carbodiimide (DCCI) in 5 mL of anhydrous CH_2-Cl_2 was slowly added. The mixture was kept under stirring at room temperature for 24 h. The precipitate formed was filtered off and the organic solution was washed with 5% HCl and 5% $NaHCO_3$ and dried over Na_2SO_4. Subsequently, the solvent was evaporated under vacuum and the crude residue was purified by silica gel column chromatography using an ethyl acetate/hexane ($^1/_3$ v/v) mixture as the eluent. Finally, the product was recrystallized from methanol giving 2.1 g (46% yield) of pure **(3)** (mp 61−62 °C).

^{1}H NMR ($CDCl_2$, δ in ppm): 1.2−1.9 (18H, aliphatic CH_2), 2.6 (2H, CH_2CF_2), 4.1 (2H, CH_2OPh), 4.2 (2H, CH_2OOCPh), 4.5 (2H, CH_2OOC), 5.8 (1H, CH = trans), 6.1 (1H, CH = gem), 6.4 (1H, CH = cis), 6.9 (2H, aromatic), 8.0 (2H, aromatic).

IR (KBr pellet, $\bar{\nu}$ in cm^{-1}) = 3100−3050 (ν C−H aromatic), 2980−2840 (ν CH_2), 1720 (ν C=O), 1680−1450 (ν C=C aromatic and vinyl), 1250−1040 (ν C−O−C), 720 (ρ CH_2), 710 (δ C−H aromatic), 645 (ω CF_2).

^{19}F NMR ($CDCl_3$, δ in ppm): −5 (3F, CF_3), −37 (2F, CF_2), −44 to −50 (12F, 6 CF_2).

Anal. Calcd ($C_{31}H_{33}F_{17}O_5$): C, 46.05; H, 4.11; F, 39.94. Found: C, 46.08; H, 4.10; F, 40.1.

Synthesis of Polyacrylates. In a typical polymerization experiment, 1.0 g of fluorinated acrylate monomer **(3)** was dissolved in 5 mL of dry trifluorotoluene in the presence of 10 mg of azobis-isobutyronitrile (AIBN) as a radical initiator. The reaction mixture was introduced into a Pyrex glass vial under nitrogen atmosphere, subjected to three freeze-pumping-thaw cycles and sealed under vacuum. After 48 h reaction at 60 °C, the polymerization mixture was poured into methanol. The solid precipitate of poly**(3)** was filtered, dissolved in 1,1,2-trifluorotrichloroethane and reprecipitated into methanol. This procedure was repeated twice before drying the polymer overnight at 60 °C under vacuum.

^{1}H NMR ($CDCl_3$, δ in ppm): 1.2−2.5 (23H, aliphatic CH_2 + CH_2CF_2 + CH_2CHCOO), 4.1 (2H, CH_2OPh), 4.2 (2H, CH_2-OOCPh), 4.5 (2H, CH_2OOC), 6.9 (2H, aromatic), 8.1 (2H, aromatic).

IR (film on KBr, $\bar{\nu}$ in cm^{-1}) = 3100−3050 (ν C−H aromatic), 2980−2840 (ν CH_2), 1720 (ν C=O), 1600−1450 (ν C=C aromatic), 1250−1040 (ν C−O−C), 720 (γ CH_2).

Table 1. Amplitudes[a] a_m of Diffraction of the Different Orders of Reflections

sample	mesophase	a_1	a_2	a_3	a_4	a_5
poly**(1)**	$S_{F2\ (or\ I2)}$	1	0	0.37	0.19	0.14
	S_{C2}	1	0	0.34	0.16	0.17
poly**(2)**	$S_{F2\ (or\ I2)}$	1	0.19	0.34	0.10	0.23
	S_{C2}	1	0.21	0.38	0.11	0.20
poly**(3)**	$S_{F2\ (or\ I2)}$	1	0.22	0.46	0.10	0.19

[a] After normalization to the amplitude value of the first-order reflection.

^{19}F NMR ($CDCl_3$, δ in ppm) −6 (3F, CF_3), −38 (2F, CF_2), −45 to −49 (10F, $5CF_2$), −52 (2F, CH_2CF_2).

Characterization of Precursors and Polymers. ^{1}H NMR and ^{19}F NMR spectra were recorded with Varian Gemini 200 and Varian Gemini VXR 300 spectrometers, respectively. Tetramethylsilane and trifluoroacetic acid were used as internal references for chemical shifts, respectively.

Gel permeation chromatography (GPC) was carried out with a Jasco PU-1580 liquid chromatograph equipped with four PL gel 5 mm Mixed-C columns, a Jasco 830-RI refractive index detector and a Perkin-Elmer LC75 UV detector. Molecular weights were referred to monodisperse polystyrene standards. $CHCl_3$ was used as a solvent at 1 mL/min flux. Volumes of 20 μL of 1 wt % polymer solution were used for GPC measurements. Light-scattering measurements were performed with a He−Ne laser source at λ = 633 nm using a Sofica 4200 photogoniometer equipped with a cylindrical cell immersed in a toluene bath. The refractive index increments were also measured with a KMX 16 laser differential refractometer at the same wavelength.

Differential scanning calorimetry (DSC) measurements were performed with a Mettler DSC-30 instrument. Samples of 5−15 mg were used with 5 to 20 °C/min heating/cooling rate. The phase transition temperatures of the monomers were extrapolated as the onset temperatures. The phase transition temperatures of the polymers were taken as the maximum temperature in the DSC enthalpic peaks. The glass transition temperature was taken as the half-devitrification temperature in the heating cycle.

Optical microscopy observations were performed on polymer powder sandwiched between glass slides. A Reichert-Jung Polyvar microscope equipped with a programmable Mettler FP52 heating stage operating at a scanning rate of 3 to 10 °C/min was used.

Wide-angle X-ray diffraction patterns were obtained with a homemade diffractometer equipped with a pinhole camera under vacuum, using Ni-filtered Cu Kα radiation. The patterns were recorded as a function of temperature using a heating device operating between 20 and 300 °C with an accuracy of ±1 °C, and especially designed to operate with capillaries containing powder or fiber samples. Several exposures were taken so as to measure the strongest and the weakest reflections. Experimental amplitudes, a_m, of diffraction for the different orders of reflections from the smectic layers were corrected for the Lorentz-polarization factor and normalized to the amplitude of the respective first order (Table 1).

Results and Discussion

Synthesis and Thermal Behavior of Polyacrylates. The polymers were prepared by the synthetic procedure outlined in Scheme 1.

Monomers **1** and **2** consisting of a phenyl benzoate mesogenic core and an alkylene spacer of different numbers n of methylene units (n = 3 or 11) were obtained in high purity by reacting 4-(perfluorooctylethoxy)phenol **(11)** with 4-(3-acryloyloxypropoxy)-benzoic acid **(7—3)** and 4-(11-acryloyloxyundecyloxy)-benzoic acid **(7—11),** respectively, using cyclohexyl carbodiimide (DCCI) as a condensing agent and pyrrolydinopyridine (PPy) as a nucleophilic activator. The above benzoic acids had been prepared starting from ethyl 4-hydroxybenzoate **(4)** as a commercial precursor via a Williamson etherification reaction with α,ω-hydroxybromoalkanes (n = 3 or 11) followed by ester cleavage and acryloylation reaction of the resulting alcohols **(6—*n*)**. 4-(Perfluorooctylethoxy)phenol **(11)** had been prepared via a Mitsunobu etherification reaction of a benzoyl mono-capped hydroquinone with perfluorooctylethanol followed by ester cleavage. Monomer **3** was synthesized by reacting commercially available perfluorooctylethanol (chemical purity 99%) with 4-(11-acryloyloxyundecyloxy)benzoic acid **(7—11)** under the same experimental conditions as for the previous monomers.

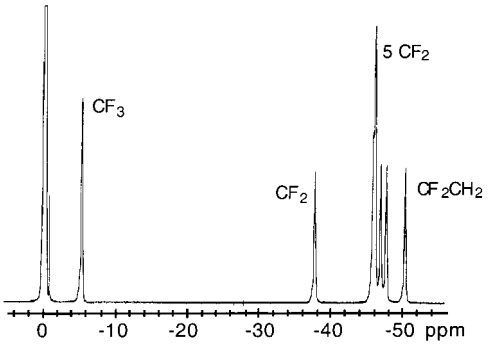

Figure 1. ^{19}F NMR spectrum of poly**(3)** (CF_3CO_2H internal reference).

Table 2. Phase Transition Temperatures and Enthalpies for Acrylate Monomers

sample	phase transition temp (°C) (ΔH (J/g) in parentheses)[a]
(**1**)	K 91 (59) S_A 177 I (15)
(**2**)	K_1 54 (7) K_2 71 (16) K_3 92 (25) [S_X 84 (9)] S_A 120 (13) I
(**3**)	K 61 (82) I

[a] K = crystalline modification; S_A = smectic A; S_X = unidentified smectic; I = isotropic. Monotropic mesophases in square brackets.

The corresponding polymers were obtained by free-radical initiation (AIBN) at 60 °C in anhydrous trifluorotoluene solution. This solvent was chosen as the reaction medium in order to delay polymer precipitation during the polymerization. The yields ranged between 60 and 70%. A ^{19}F NMR spectrum is illustrated for poly-**(3)** in Figure 1. Molar masses of poly**(1)** and poly**(2)** were not determined because of insolubility of the polymers in common solvents. Poly**(3)** showed an M_n of 40000 and an M_w/M_n of 1.7 as determined by gel permeation chromatography (and an M_w of 75000 by light-scattering measurements).

The phase transition temperatures and relevant thermodynamic parameters of monomers and polymers were determined by DSC measurements, and the liquid-crystalline behavior was elucidated by polarizing microscopy. All the samples were previously heated to a temperature higher than the isotropization point in order to cancel any effect of the former thermal history on phase transitions. Monomers **1** and **2** formed a smectic A (S_A) mesophase that transformed into the isotropic state at 177 and 120 °C, respectively (Table 2). An additional monotropic smectic mesophase occurred in **2** at 84 °C. In contrast, monomer **3** gave rise to no mesophase.

Polymers poly**(1)** and poly**(2)** had a qualitatively similar thermal behavior which however was quite different from poly**(3)**, due to the different chemical

Table 3. Transition Temperatures and Enthalpies for Liquid-crystalline Polyacrylates

sample	phase transition temp (°C)[a] (ΔH (J/g) in parentheses)
poly**(1)**	G 100 $S_{F2\ (or\ I2)}$ 144 (7.2) S_{C2} 197 (2.1) S_X 260 dec[b]I
poly**(2)**	G 70 $S_{F2\ (or\ I2)}$ 126 (7) S_{C2} 210 (14.4) I
poly**(3)**	G 27 $S_{F2\ (or\ I2)}$ 76 (25) N 99 (2.8) I

[a] G = glass, S = smectic, S_X = unidentified smectic, N = nematic, I = Isotropic. [b] With thermal decomposition.

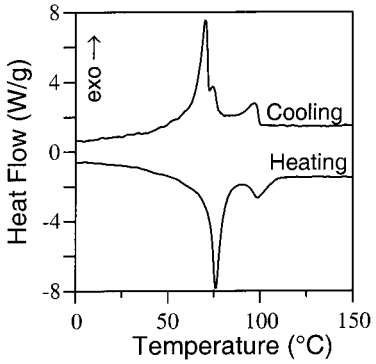

Figure 2. DSC traces of polymer poly**(3)** (scan rate of 10 °C/min).

Figure 3. Optical micrograph of the fan-shaped texture of poly**(3)** at 93 °C (original magnification 320×).

structure of the side chains of the two types of polymers (Table 3).

The glass transition temperature (T_g) decreased passing from 100 °C for poly**(1)** to 27 °C for poly**(3)**, which would be consistent with an increased flexibility of the polymer backbone that was decoupled from the side chains by a longer flexible spacer in the latter polymers. Several first-order transitions in the DSC curves were attributed to the phase transitions between different mesophases (Figure 2). The liquid-crystal range was especially broad for poly**(1)** ($T_i - T_g > 160$ °C), even though the isotropization temperature (T_i) could not be unequivocally detected because of partial thermal degradation of the polymer.

It is worth noting that poly**(3)** containing one phenyl ring per side chain presented liquid-crystal behavior ($T_i - T_g = 72$ °C) even in a polymorphic sequence. A fanlike texture was exhibited by the low temperature mesophase which was accordingly identified as smectic (Figure 3).

X-ray Studies of Polyacrylates. X-ray diffraction measurements were carried out on powder samples of the polymers in order to identify the encountered

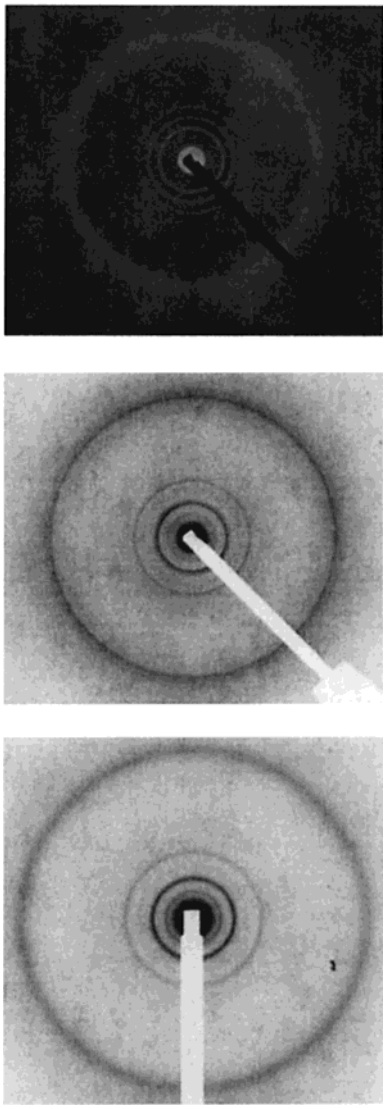

Figure 4. X-ray diffraction patterns of poly**(1)** at 25 °C (top), poly**(2)** at 80 °C (center), and poly**(3)** at 60 °C (bottom).

mesophases. The diffraction patterns at room temperature presented five low-angle Bragg reflections with periodicities in the ratio 1:2:3:4:5 for poly**(2)** and poly**(3)**, or four reflections with periodicities in the ratio 1:3:4:5 for poly**(1)** (Table 1), indicative of a layered, smectic structure (Figure 4). The patterns also showed one sharp and intense reflection at wide angles, which allowed identification of a hexatic smectic mesophase with a pseudohexagonal lattice[29] of side a of about 5 Å (Table 4). The determined layer periodicity d compared to the length L of the repeat unit, as calculated in the hypothesis of an extended planar conformation of the side chain with the fluorocarbon segment in a twisted zigzag conformation of span $p = 2.59$ Å,[30] suggested that the side chains were organized in either a partially interdigitated structure (S_{Bd}) or a tilted, double layer structure (S_{F2} or S_{I2}). Our investigations into the electron density profiles of the smectic mesophases helped us conclude that their structure was indeed tilted, double layer (see below).

Schematic representations of the in-plane packing of the molecules in S_{F2} and S_{I2} smectics are shown in Figure 5. In both cases the mesogens are organized in a pseudohexagonal lattice, which is tilted toward the side of the hexagon in the smectic F and toward the apex

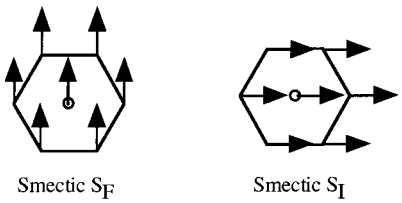

Figure 5. Schematic representation of the in-plane order in S_F and S_I mesophases (top view; the arrows point to the tilt direction).

Table 4. Structural Parameters of the Different Mesophases of the Liquid-Crystalline Polyacrylates

mesophase	param	poly**(1)**	poly**(2)**	poly**(3)**
	L (±1 Å)	33	43	37
$S_{F2\ (or\ I2)}$	d (±0.3 Å)	54.8	72.5	63.2
	a (±0.1 Å)	5.2	5.7	5.3
	θ (±1°)	27	28	24
S_{C2}	d (±0.3 Å)	52.7	70.3	
	D (±0.1 Å)	4.9	5.1	
	θ (±1°)	31	31	

of the hexagon in the smectic I.[31] There is a greater in-plane correlation length in the S_I than in the S_F phase.[31,32] However, the subtle differences in the tilt direction of the molecules in the two mesophases makes it very difficult to recognize them, unless they are formed successively in a polymer.[33] Their exact nature, either F or I, could not be attributed in our cases. The relevant structural parameters are collected in Table 4. For example, for poly**(1)** $d = 54.8$ Å and $L = 32.7$ Å, which would correspond to a maximum tilt angle $\theta = 27°$.

On heating, poly**(1)** and poly**(2)** underwent a phase transition to another smectic mesophase; see Table 3 for phase transition temperatures and enthalpies. Such smectic mesophase was a disordered one, as demonstrated by the detection in their diffraction patterns of a diffuse halo at wide angles along with four or five low-angle sharp reflections (Figure 6). This is characteristic of a mesophase lacking long-range correlation between the side chains that are assembled in liquidlike layers. An intermolecular distance D of ca. 5 Å was evaluated. The comparison between the determined d and the calculated L evidenced that the side chains were organized in a tilted, double layer structure (S_{C2}). For poly**(1)**, $d = 52.7$ Å that corresponded to a tilt angle $\theta = 31°$.

Therefore, the layer spacing decreased, and accordingly the tilt angle increased, in passing from the hexagonal smectic mesophase to the disordered smectic mesophase. This particular feature is rather uncommon for liquid crystals, in which normally either less tilted or orthogonal mesophases are originated at higher temperatures above tilted mesophases,[34] the most frequent and best known such phase transition being the smectic C-to-smectic A transition with rising temperature. The layer thickness remained unaffected by temperature within the whole range of stability of each smectic mesophase, whether ordered or disordered, an abrupt decrease of d being detected at the phase transition temperature only.

Whereas in poly**(2)** the disordered smectic mesophase persisted up to the phase transition to the isotropic melt at $T_i = 210$ °C, poly**(1)** gave rise to a third mesophase above 197 °C, whose nature could not be identified because of the occurrence of decomposition of the sample during the experiments at the high temperatures. In contrast, poly**(3)** formed a nematic mesophase above its hexagonal smectic mesophase as proven by the X-ray patterns exhibiting a diffuse wide-angle halo only (Figure 6). The direct transition from an ordered smectic to the nematic is rare,[34] in that between these phases most frequently different intermediary phases intervene which possess a lower degree of order before reaching the least ordered high-temperature, viz. nematic, mesophase. Such a phase transition entailed a substantial disruption of the orderly packing of the mesogenic side chains, which manifested in the significant changes in enthalpy ($\Delta H = 25$ J/g) and entropy ($\Delta S = 7.2 \times 10^{-2}$ J/g K) associated with it in poly**(3)**. This finding is likely due to the comparatively weak mesogenic character of these one-phenyl fluorinated side chains, whose positional correlation in smectic layers easily breaks down (at 76 °C).

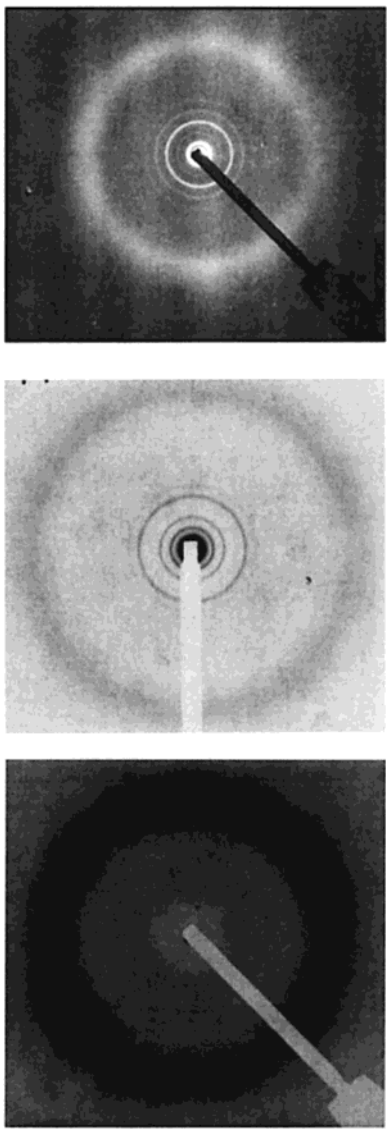

Figure 6. X-ray diffraction patterns of poly**(1)** at 153 °C (top), poly**(2)** at 130 °C (center), and poly**(3)** at 80 °C (bottom).

It was not possible to draw oriented fibers from the melt phase of the polymers, and the nature of the mesophases could not be ascertained by this means. However, this was achieved by studying their electron density profiles.

Electron Density Profiles. The detection of as many as up to five low-angle orders of reflections in the

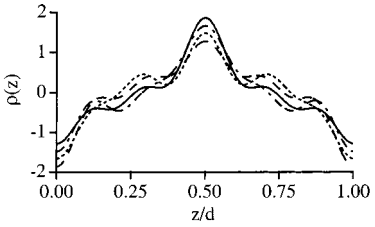

Figure 7. Electron density profiles $\rho(z)$ of the low-temperature mesophase of poly**(2)** for the combinations of signs -+-+- (—), - - -+- (...), -+- - - (_._), and - - - - - (- - -) (the other four symmetrical profiles are not shown).

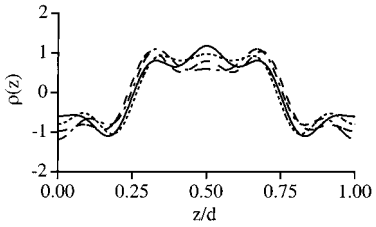

Figure 8. Electron density profiles $\rho(z)$ of the low-temperature mesophase of poly**(2)** for the combinations of signs -+++- (—), -++- - (...), - -+- - (_._), and - -++- (- - -) (the other four symmetrical profiles are not shown).

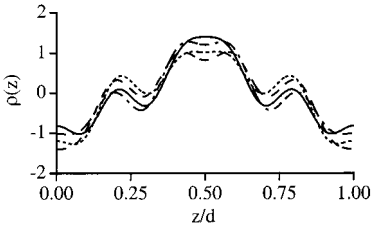

Figure 9. Electron density profiles $\rho(z)$ of the low-temperature mesophase of poly**(2)** for the combinations of signs -+-++ (—), - - -++ (...), -+- -+ (_._), and - - - -+ (- - -) (the other four symmetrical profiles are not shown).

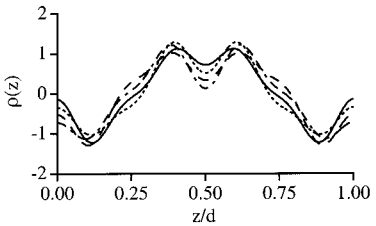

Figure 10. Electron density profiles $\rho(z)$ of the low-temperature mesophase of poly**(2)** for the combinations of signs -++++ (—), -++-+ (...), - -+-+ (_._), and - -+++ (- - -) (the other 4 symmetrical profiles are not shown).

X-ray patterns clearly showed that the modulation of the elctron density along the layer normal was not simply sinusoidal[35] and could allow detailing the structural order within the smectic layers of the polymers. Accordingly, we evaluated the electron density profiles $\rho(z)$ along the layer normal of the smectic mesophases. The layer normal is parallel to the mesophase director in orthogonal mesophases, like S_{Bd} and S_{Ad}, or otherwise it is inclined by an angle θ with respect to the director in tilted mesophases, like S_{F2} and S_{C2}. Owing to the centrosymmetry of the above structures, the electron density profile $\rho(z)$ was given by eq 1[36]:

$$\rho(z) = \sum a_m \cos(m2\pi z/d) \qquad (1)$$

As experimentally the intensities of the reflections were measured, the signs of the structure factors a_m were lost, and therefore 2^m electron density profiles were obtained for the various combinations of signs of a_m, where m represents the number of low-angle reflections.[33,35]

Model electron density profiles were derived for each polymer in the tilted and in the orthogonal mesophases by calculating the average electron density ρ of each part of the repeat unit by dividing its number of electrons by its length measured with the CPK models ($\rho = 6.4$ e/Å for $(CH_2)_{11}$, $\rho = 16.1$ e/Å for $O(CH_2)_2(CF_2)_8F$, $\rho = 9.2$ e/Å for C_6H_4CO, and $\rho = 9.2$ e/Å for CH_2CHCOO). The electron density profile for a tilted, double layer structure should present a central rather deep minimum flanked by two prominent maxima corresponding to the fluorinated tails, two secondary maxima deriving from the phenyl rings, two minima corresponding to the aliphatic spacers and two maxima due to the polymer backbones. On the other hand, the electron density profile for an orthogonal interdigitated structure would exhibit a very high central maximum corresponding to the partly overlapping fluorinated tails, two secondary maxima coming from the phenyl rings, two minima corresponding to the aliphatic spacers, and two maxima corresponding to the main chains.

As one example, we discuss the electron density profiles derived from the intensities of the low-angle reflections in the low-temperature mesophase of poly-**(2)**. There were five orders of reflections ($m = 5$), which resulted in 32 profiles $\rho(z)$. We only present 16 profiles in Figures 7−10, because the other symmetrical 16 profiles were clearly physically unacceptable.

The profiles in Figure 7 exhibited two minima for the main chains ($z/d = 0$ and 1) and therefore were rejected because they did not match any of the model profiles. The profiles in Figures 8 and 9 were also discarded since they showed either a weak maximum (Figure 8) or a shallow minimum (Figure 9) in the middle of the layer ($z/d = 0.5$) in addition to rather low values for the main chains. Finally, the electron density profiles in Figure 10 exhibited a relatively deep minimum in the middle of the layer flanked by two maxima for the fluorinated tails as well as by two shoulders for the phenyl rings ($z/d \approx 0.25$ and 0.75), two minima for the aliphatic spacers, and two secondary maxima for the polymer backbones. Any of these last four profiles was in agreement with the tilted bilayer model. There were no experimental profiles even resembling that expected for an interdigitated structure.

Very similar electron density profiles were evaluated for the high-temperature smectic mesophase with minor differences in the relative profile intensities, as could be expected in consideration of the small differences in the values of a_m detected in each mesophase. This provided clear arguments in favor of the existence of a tilted, double layer mesophase at high temperatures for poly**(2)**. Analogous considerations applied to the other polymers (compare a_m values in Table 1). Consequently, the occurrence of any orthogonal phases was ruled out and we concluded that the encountered mesophases were S_{F2} (or S_{I2}) for each of the three polymers at low temperatures, and S_{C2} for poly**(1)** and poly**(2)** at high temperatures.

Fluorocarbon chains are known to adopt a helical conformation in the solid state, which is preserved in the mesophase.[18,30] This confers to them a rodlike character suitable for mesophase formation when incorporated into an appropriate molecular framework, and special conformational changes of these segments

can effect phase transitions in the molecules incorporating them.[37] The terminal CF_3 group of these rodlike chains such as those in the present polymers is rather bulky with a van der Waals volume of the equivalent hemisphere of 42.6 Å^3 (compare with 16.8 Å^3 for the CH_3 group)[38,39] and a cross-section surface of 23 Å^2 as estimated by molecular models. It appears, therefore, that there would be an excessive steric hindrance for two antiparallel fluorinated tails to overlap and to order within the layers of an interdigitated smectic phase. Conversely, an efficient space filling can be realized by the side chains by tilting the fluorinated tails in an end-to-end arrangement of a double layer smectic structure, e.g. S_{F2} and S_{C2}. Such structures seem to be preferred in the present class of polyacrylates. This may be favored by the presence of a short $(CH_2)_2$ segment bridging the fluoroalkyl tail to the aromatic moiety.

Conclusions

New polyacrylates containing the 4-(perfluorooctylethoxy)phenyl benzoate and 4-perfluorooctylethyl benzoate groups in the side chains were synthesized. All the polymers displayed a polymorphic liquid-crystalline behavior, that especially included a very unusual hexatic smectic-to-nematic phase sequence for poly**(3)**, bearing a one-phenyl core in the side chains. This structure per se would not be able to promote formation of a mesophase because of its inherently insufficient aspect ratio, which indeed is offset by attachment of a fluorinated rodlike tail substituent. Furthermore, phase separation on a molecular scale of the aliphatic−aromatic−fluoroaliphatic components of the polymer side chains can stabilize their orderly packing in different sublayers of smectic mesophases.

One anticipates that the surface structure of a thin polymer film might be different from the bulk structure, in particular for the packing in the outer few layers toward the polymer−air (or water) interface. Investigations on the surface order and structure of the polyacrylate films are in progress.

Acknowledgment. The authors thank Prof. Emo Chiellini for many invaluable discussions. Partial financial support from the Italian Ministry for the University and Scientific Research (MURST) is also gratefully acknowledged.

References and Notes

(1) Volkov, V. V.; Platé N. A.; Takahara, A.; Kajiyama, T.; Amaya, M.; Murata, Y. *Polymer* **1992**, *33*, 1316.
(2) Percec, V.; Lee M. *J. Macromol. Sci. Pure Appl. Chem.* **1992**, *A29*, 723.
(3) Wilson, L. M.; Griffin, A. C. *Macromolecules* **1994**, *27*, 1928.
(4) Beyou, E.; Babin, P.; Bennetau, B.; Dunogues, J.; Teyssie, D.; Boileau, S. *J. Polym. Sci., Part A, Chem. Ed.* **1994**, *32*, 1673
(5) Krupers, M.; Möller, M. *Macromol. Chem. Phys.* **1997**, *198*, 2163.
(6) Wang, J.; Mao G.; Ober, C. K.; Kramer, J. E. *Macromolecules* **1997**, *30*, 1906.
(7) Wang, J.; Ober, C. K. *Macromolecules* **1997**, *30*, 7560.
(8) Bracon, F.; Guittard, F.; Taffin de Givenchy, E.; Cambon, A. *J. Polym. Sci., Part A: Polym. Chem.* **1999**, *37*, 4487.
(9) Xiang, M.; Li X.; Ober, C. K.; Char, K.; Genzer, J.; Sivaniah, I.; Kramer, E. J.; Fischer, D. A. *Macromolecules* **2000**, *33*, 6106.
(10) Scheirs, J., Ed. *Modern Fluoropolymers*; Wiley: Chichester, U.K., 1997.
(11) Mahler, W.; Guillon, D.; Skoulios, A. *Mol. Cryst. Liq. Cryst. Lett.* **1985**, *2*, 111.
(12) Viney, C.; Twieg, R. J.; Russel, T. P.; Depero, L. E. *Liq. Cryst.* **1989**, *5*, 1783.
(13) Viney, C.; Twieg, R. J.; Gordon, B. R.; Rabolt, J. F. *Mol. Cryst. Liq. Cryst.* **1991**, *198*, 285.
(14) Wilson, L. M. *Macromolecules* **1995**, *28*, 325.
(15) Napoli, M. *J. Fluorine Chem.* **1996**, *79*, 59.
(16) Semenov, A. M.; Vasilenko, S. V. *Serv. Phys. JEPT*, **1985**, *63*, 70.
(17) Bunn, C. W.; Howells, E. R. *Nature (London)* **1954**, *174*, 549.
(18) Russell, T. P.; Rabolt, J. F.; Twieg, R. J.; Siemens, R. L.; Farner, B. L. *Macromolecules*, **1986**, *19*, 1135.
(19) Demus, D., Goodby, J., Gray, G. W., Spiess, H.-W., Vill, V., Eds. *Handbook of Liquid Crystals*; Wiley-CH: Weinheim, Germany, 1998; Vols. 2A and 2B.
(20) Nguyen, H. T.; Sigaud, G.; Achard, M. F.; Hardouin, F.; Twieg, K.; Betterton, R. J. *Liq. Cryst.* **1991**, *10*, 389.
(21) Liu H.; Nohira, H. *Liq. Cryst.* **1997**, 22, 217.
(22) Chen, B.-Q.; Yang, Y.-G.; Wen J. X. *Liq. Cryst.* **1998**, *24*, 539.
(23) Chen, B.-Q.; Yang, Y.-G.; Wen J. X. *Liq. Cryst.* **1999**, *26*, 1135.
(24) Taffin de Givenchy, E.; Guittard, F.; Bracon, F.; Cambon, A. *Liq. Cryst.* **1999**, *26*, 1107.
(25) Taffin de Givenchy, E.; Guittard, F.; Bracon, F.; Cambon, A. *Liq. Cryst.* **1999**, *26*, 1095.
(26) Okamoto, H.; Yamada, N.; Takenaka, S. *J. Fluorine Chem.* **1998**, *91*, 125.
(27) Okamoto, H.; Petrov, V. F.; Takenaka, S. *Bull. Chem. Soc. Jpn.* **1999**, *72*, 1637.
(28) Wynne, K. J.; Nissan, R. A. *Macromolecules* **1993**, *5*, 1299.
(29) De Vries, A. *Mol. Cryst. Liq. Cryst.* **1985**, *131*, 125.
(30) Davidson, T.; Griffin, A. C.; Wilson, L. M.; Windle, A. H. *Macromolecules* **1995**, *28*, 354.
(31) Gane, P. A. C.; Leadbetter, A. J.; Benattar, J. J.; Moussa, F.; Lambert, N. *Phys. Rev. A* **1981**, *24*, 2694.
(32) Benattar, J. J.; Moussa, F.; Lambert, N. *J. Phys. (Paris) Lett.* **1981**, *42*, L67.
(33) Gallot, B.; Galli, G.; Ceccanti, A.; Chiellini, E. *Polymer* **1999**, *40*, 2561.
(34) Gray, G. W.; Goodby, J. W. *Smectic Liquid Crystal*; Leonard Hill: Glasgow, Scotland, 1984.
(35) Davidson, P.; Levelut, A. M.; Achard, M. F.; Hardouin, F. *Liq. Cryst.* **1989**, *4*, 561.
(36) Gudkov, V. A. *Sov. Phys. Crystallogr.* **1984**, *29*, 316.
(37) Wang, J.; Ober, C. K. *Liq. Cryst.* **1999**, *26*, 637.
(38) Seebach, D. *Angew. Chem., Int. Ed. Engl.* **1990**, *29*, 1320.
(39) Bondi, A. *J. Phys. Chem.* **1964**, *68*, 44.

MA010728F